400-G Single Carrier 500-km Transmission With an InP Dual Polarization IQ Modulator

Mohammed Y. S. Sowailem, Thang M. Hoang, Mohamed Morsy-Osman, Mathieu Chagnon, David Patel, Stephane Paquet, Carl Paquet, Ian Woods, Odile Liboiron-Ladouceur, *Senior Member, IEEE*, and David V. Plant, *Fellow, IEEE*

***Abstract*— In this letter, we demonstrate experimentally 400-G transmission over 500 km using an InP-based dual-polarization IQ modulator on a single wavelength. The results show that a 56-Gbaud polarization division multiplexed (PDM)-16-quadratic-amplitude modulation (QAM) modulated signal can be transmitted over 500 km at a bit error rate (BER) below the hard decision forward error correcting threshold of 3.8×10^{-3}. A 43-Gbaud PDM-64-QAM modulated signal can be transmitted over 320 km with a BER below the soft decision forward error correcting threshold of 2×10^{-2}.**

***Index Terms*— Coherent system, digital signal processing, indium phosphide based modulator, modulation formats.**

I. Introduction

CONTINUOUS increase in data rate requirements especially for short reach and metro applications is creating significant demand for 400G capable systems. There are several approaches to achieve this high data rate. One approach is to use high symbol rates and low order modulation formats. For example, a super-Nyquist filtered 110 Gbaud polarization division multiplexed (PDM)-QPSK signal is used to reduce the signal bandwidth to 100 GHz [1]. Another approach is to use higher order modulation formats including 16-QAM [2], [3], or 64-QAM [4], and operate at lower symbol rates. All of these approaches require digital signal processing (DSP) at the transmitter and the receiver (some is done in the optical domain as in [3]). Another approach is to use either wavelength division multiplexing, for example dual-carrier 32 Gbaud PM-16-QAM [5], or time division multiplexing [6]. Current challenges include realizing high data rate systems implemented using reduced complexity transmitters. InP-based Mach-Zhender modulators (MZMs) operating at low voltages with reported values of V_π ranging from 1 to 2.5 V are a viable technology option [7]–[9]. Also, InP-based devices can be integrated with lasers [7], RF amplifiers [9] and SOAs [10].

Several single carrier transmission demonstrations have been reported that utilize InP-based IQ modulators operating over varying distances, data rates, and modulation formats. In [7], the authors demonstrated long haul transmission at 32 Gbaud PDM-QPSK and PDM-16-QAM over 8000 km, and 960 km, respectively. In [11], a 28 Gbaud 64-QAM modulated signal is transmitted over 40 km at a BER of 1.0×10^{-2}.

In this letter, we demonstrate 400G transmission using a 2.5V V_π InP-based dual-polarization IQ modulator (DP-IQM) on a single carrier using 16-QAM at 56 Gbaud, and 64-QAM at 38 Gbaud, and 43 Gbaud. These modulation schemes enable 400G transmission after overhead removal. To achieve this result, we implement DSP at the transmitter and the receiver, as will be discussed later, including transmitter frequency response equalization, non-linear compensation for MZM response, and other DSP algorithms. Also, an experimental comparison is performed between an InP-based and a $LiNbO_3$ based DP-IQM. The remainder of the letter is organized as follows: Section II is dedicated to the DP-IQM description. Section III discusses the experimental setup and the DSP functions. Section IV presents the experimental results, and we conclude in Section V.

II. InP-Based DP-IQM

InP-based modulators offer a significant size reduction compared to $LiNbO_3$ modulators due to larger phase-voltage efficiency per unit length attributed to the Quantum Confined Stark Effect. The DP-IQM used in this experiment is packaged in a 41 mm by 19 mm module and uses two InP chip-on-carriers as described in [8]. Fig. 1 shows a schematic illustrating the DP-IQM design. The input optical power is collimated and split between the two InP chips using a free-space micro-optic 3 dB splitter. A standard aspheric lens is used to focus the light into the InP waveguide and a spot size converter integrated into the modulator was designed to reduce the coupling losses at the waveguide interface. Each InP chip has two nested MZ structures having co-planar slot-line, series push-pull travelling-wave electrodes designed for high-speed RF modulation. Phase bias and substrate bias controls are also required to set operating points and maintain constant modulation voltage over wavelength, respectively. The optical modulated signal coming out of the Y-polarization chip is rotated by 90° before being combined with the X-polarization

Manuscript received October 12, 2015; revised February 1, 2016; accepted February 17, 2016. Date of publication February 18, 2016; date of current version April 5, 2016. This work was supported by TeraXion, Inc. *(Mohammed Y. S. Sowailem and Thang M. Hoang contributed equally to this work.)*

M. Y. S. Sowailem, T. M. Hoang, M. Chagnon, D. Patel, O. Liboiron-Ladouceur, and D. V. Plant are with McGill University, Montreal, QC H3A 2A7, Canada (e-mail: mohammed.sowailem@mail.mcgill.ca; thang.hoang@mail.mcgill.ca; mathieu.chagnon@mail.mcgill.ca; david.patel@mail.mcgill.ca; odile.liboiron-ladouceur@mcgill.ca; david.plant@mcgill.ca).

M. Morsy-Osman is with McGill University, Montreal, QC H3A 2A7, Canada, and also with the Department of Electrical Engineering, Alexandria University, Alexandria 21526, Egypt (e-mail: mohamed.osman2@mail.mcgill.ca).

S. Paquet, C. Paquet, and I. Woods are with TeraXion, Inc., Quebec City, QC G1P 4S8, Canada (e-mail: spaquet2@teraxion.com; cpaquet@teraxion.com; iwoods@teraxion.com).

Color versions of one or more of the figures in this letter are available online at http://ieeexplore.ieee.org.

Digital Object Identifier 10.1109/LPT.2016.2532238

M. Y. S. Sowailem et al., "400-G Single Carrier 500-km Transmission With an InP Dual Polarization IQ Modulator," IEEE Photonics Technology Letters, vol. 28, no. 11, pp. 1213-1216, June1, 1 2016.
doi: 10.1109/LPT.2016.2532238 Reprinted with permission from IEEE

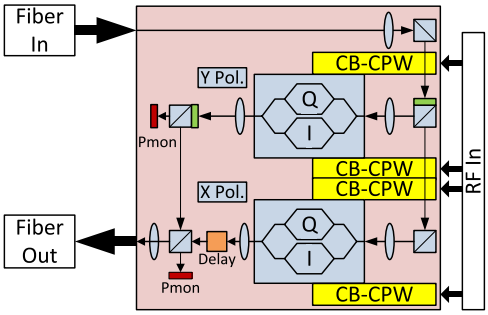

Fig. 1. InP-based DP-IQM schematic.

signal using a micro-optic polarization combiner. The X-polarization path shows an optical delay component necessary to equalize the optical path between both polarizations to limit the skew to less than 5 ps. The combination of the X and Y signals is collimated and focused inside a standard SMF fiber at the output.

The modulator exhibits an insertion loss below 10 dB and a X/Y imbalance of better than 1 dB over the C-band. The V_π for this design is 2.5V and the 3 dB bandwidth is greater than 35 GHz for all the MZ structures.

III. Experimental Setup and DSP Stack

A. Experimental Setup

Fig. 2 shows the experimental setup deployed to demonstrate the performance of the DP-IQM. An AC-coupled 8-bit digital-to-analog converter (DAC), operated at 65.7 GSps, generates four 1.2 Vpp differential outputs at the maximum output voltage swing. The four differential outputs are connected to four differential inputs of a quad linear amplifier which produces four 5 Vpp single-ended signals used to drive the DP-IQM. The optical source is a 100 kHz linewidth external cavity laser (ECL) operating at 1550.12 nm with 15.5 dBm optical power.

After modulation, the optical signal is amplified with a booster to a fixed average power of approximately 23 dBm. The booster is followed by a variable optical attenuator (VOA) used to adjust the launched power of the signal to its optimum value according to the modulation format and symbol rate used. The signal is then launched into an optical re-circulating loop containing four spans. Each span contains 80 km of SMF-28e+ followed by an inline erbium-doped fiber amplifier (EDFA) with 5 dB noise figure. The second span is followed by a tunable filter with the center wavelength at 1550.12 nm and bandwidth of 2 nm.

The output signal from the re-circulating loop is coupled with a noise signal using a 3-dB coupler for characterization purposes. The noise loading is done using an amplified spontaneous emission (ASE) noise source followed by a VOA to control the optical signal-to-noise ratio (OSNR). The output of the 3-dB coupler is followed by a 99% coupler with the 1% port connected to an optical spectrum analyzer (OSA) for OSNR measurements. The 99% port is connected to a 0.8 nm filter followed by pre-amplifier and a second VOA. The optimum received power determined experimentally is 7.4 dBm. This high input power is required in order to compensate for

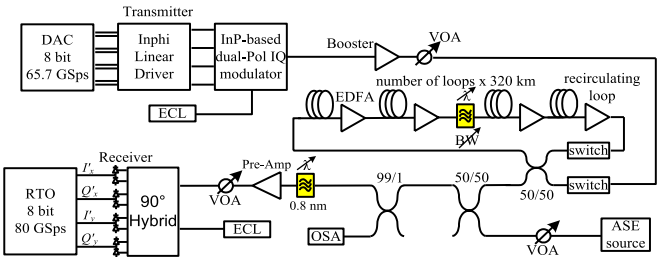

Fig. 2. Experimental setup.

the 10 dB loss of the optical hybrid, thus insuring adequate received optical power. A 15.5 dBm, 100 kHz linewidth ECL operating at 1550.12 nm is used as a local oscillator laser. The optical hybrid is followed by four balanced detectors feeding a 33 GHz, 8-bit, real time oscilloscope (RTO) operating at 80 GSps for offline signal processing.

B. DSP Stack

Fig. 3 illustrates the DSP stack used at the transmitter and receiver. The transmitter DSP (Tx-DSP) starts with N-QAM symbol generation, generating four random streams for dual polarization transmission. Each stream is uniformly distributed over M levels where $M = \log_2(N)$. Next, the generated symbols are pulse shaped using a root-raised-cosine (RRC) filter at 2 samples per symbol. The roll-off factors used in the RRC filter for 56, 43, 38 Gbaud signals are 0.1, 0.4, and 0.5, respectively. Next, the four streams are re-sampled to the 65.7 GSps sampling rate of the DAC. This is followed by clipping and non-linear compensation for the MZM transfer function which is needed in order to have equally-spaced constellation points after optical modulation. Then, an equalizing filter is used to compensate for the frequency response of transmitter components including (i) the DAC (3-dB bandwidth of 13 GHz), (ii) the quad linear driver (3-dB bandwidth of 30 GHz), and (iii) the DP-IQM (3-dB bandwidth of 35 GHz). Compensation of the overall frequency roll-off of the transmitter minimizes the RF swing out of the DAC. This results in a lower RF signal swing applied to the DP-IQM via the quad linear driver. Therefore there is a trade-off between the amount of transmitter frequency response compensation applied at the transmitter versus the RF input swing applied to the DP-IQM. The transmitter equalizing filter is experimentally optimized at each symbol rate. The transmitter frequency response compensation is followed by signal quantization to 256 levels for the 8-bit DAC.

The receiver DSP (Rx-DSP) starts with IQ power imbalance compensation and quadrature error correction using Gram-Schmidt orthogonalization [12]. Next, the data is re-sampled from 80 GSps to double the symbol rate. After re-sampling, frequency domain chromatic dispersion (CD) compensation is performed [13] followed by frequency offset removal using the periodogram method [14]. Then, matched filtering is done followed by a timing recovery to select the appropriate sampling instance [15]. Clock recovery is not required because a common reference clock is supplied to the DAC and RTO. Next, synchronization is performed using a cross-correlation between the received symbols captured

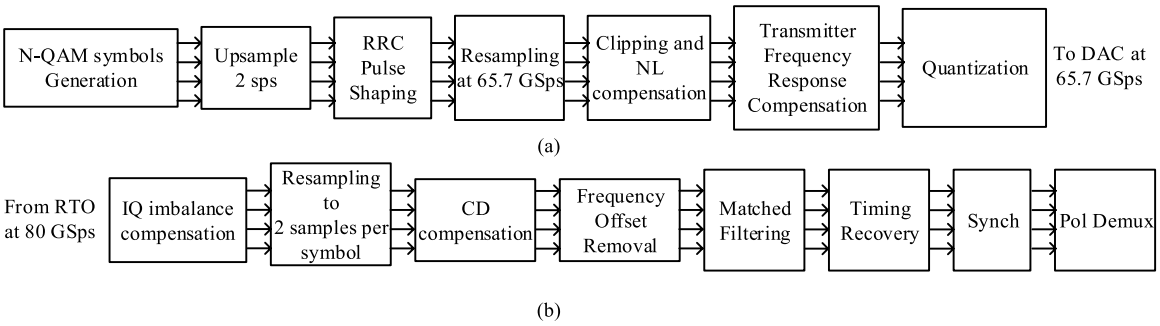

Fig. 3. DSP stack used for the transmission: (a) Tx-DSP; (b) Rx-DSP.

by the RTO and the training symbols. Initial polarization tracking is done using the training symbol least mean squares (TS-LMS) algorithm [16]. After initial convergence, decision directed LMS (DD-LMS) for steady-state operation is used. Finally, phase noise and residual frequency offset are mitigated by a second order phase locked loop (PLL) [17] that is included within the TS- and DD-LMS algorithms.

IV. Results

Fig. 4(a) shows the BER versus transmission distance for a 56 Gbaud 16-QAM signal at different launched powers. After sweeping the launched power, we found that the optimum launched power is 3 dBm for all transmission distances. At the optimum launched power, 448 Gbps can be transmitted over 500 km while operating below the HD-FEC threshold. Also, at 0 km, which is a back-to-back (B2B) configuration with no noise loading, we measure a non-zero BER floor of 2.4×10^{-4}.

Next, Fig. 4(b) shows the BER versus OSNR in 0.1 nm bandwidth for the 56 Gbaud 16-QAM signal measured using noise loading in B2B configuration. In addition, we plot the theoretical BER vs. OSNR curve which assumes white Gaussian noise is added on an otherwise noise free undistorted signal. We also include the measured B2B BER floor of 2.4×10^{-4} at an optimum launch power of 3 dBm taken from Fig. 4(a). Because of the presence of this noise floor we conclude that the experimental OSNR curve at large OSNR values ($\sim>$ 40 dB) will converge to this 2.4×10^{-4} BER value. Furthermore at these high OSNR values the system is operating with very low optical noise because there is no optical noise loading in this configuration. Hence, we conclude that this BER floor is caused by the electrical noise in our system, and that the dominant contribution to this noise is the in-band transmitter electrical noise power. The result is the observed 5 dB implementation penalty between measured and theory curves at HD-FEC. This measured implementation penalty is consistent with recent reports of 16QAM systems operating at similar symbol rates [19], [20].

Regarding the origins of the transmitter electrical noise, the dominant contributions to this electrical noise lying within the signal bandwidth are the DAC, and the RF amplifiers. Contributions to the noise generated by the DAC include: digital waveform clipping, quantization noise, and decreasing effective number of bits (ENoB) with increasing frequency. Further, the RF amplifiers generate thermal noise. In addition generating the IQM drive signals requires pre-emphasis DSP at the transmitter in order to pre-compensate the linear system responses of the components which have limited bandwidths. The resulting signal swing from the DAC post DSP is reduced significantly. Hence, the separation between the four levels used to generate 16 QAM signals is very small. This separation will be further reduced when generating eight level signals used in 64 QAM formats. This low amplitude signal, which includes excess electrical noise as per above, is amplified by the high gain RF amplifier which adds additional noise. Finally, the large bandwidth of a 56 Gbaud signal integrates large amounts of in-band electrical noise.

Next, Fig. 4(c) shows the BER versus transmission distance at optimum launched power of 2 dBm for both 38 Gbaud 64-QAM and 43 Gbaud 64-QAM signals both delivering 400G with HD-FEC and SD-FEC overheads, respectively. We observe that using 64-QAM modulation format limits the transmission distance compared to 16-QAM. Using 38 Gbaud 64-QAM, the maximum reach is limited to 150 km at HD-FEC. The shorter reach for 64-QAM compared to 16-QAM can be explained by comparing the required OSNR in B2B at HD-FEC in Figs. 5 and 4(b) for both 38 Gbaud 64-QAM and 56 Gbaud 16-QAM, respectively. We observe that an OSNR of around 32 dB is required at HD-FEC for 38 Gbaud 64-QAM (Fig. 5) as opposed to only 27 dB for 56 Gbaud 16-QAM (Fig. 4(b)).

Finally in Fig. 5, the B2B BER versus OSNR system performance while operating at 38 Gbaud 64-QAM is reported for a 35 GHz InP and a 27 GHz $LiNbO_3$ DP-IQM. This head-to-head comparison between the two DP-IQM is performed by removing the InP-based DP-IQM in Fig. 2 and installing $LiNbO_3$ DP-IQM and then optimizing the pre-emphasis filter. We choose this symbol rate, which ensures 400G raw data rate, in order to make a proper comparison between the two platforms such that the impact of the difference in the bandwidth between the two modulators on the system performance is minimized (we use an RRC pulse at 38 Gbaud with a roll-off factor 0.5 which ensures that approximately 91% of the signal energy is confined below 19 GHz). We observe in Fig. 5 a difference of approximately 0.3 dB between the performance of the InP modulator and the $LiNbO_3$ modulator in favor of the InP modulator. In addition we observe $\sim$6 dB implementation penalty relative to theory for both modulators, the explanation for which is given above when detailing the 56 Gbaud results.

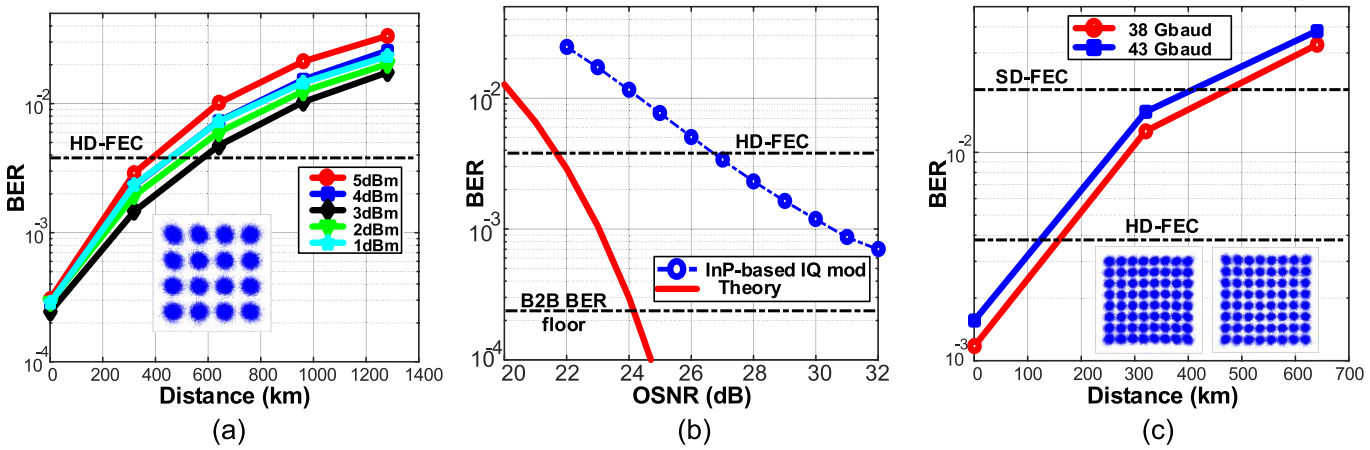

Fig. 4. (a) 56 Gbaud 16-QAM BER versus distance per launched power with B2B constellation shown. (b) BER versus OSNR for 56 Gbaud 16-QAM. (c) BER versus distance for 38 Gbaud and 43 Gbaud with B2B constellations shown.

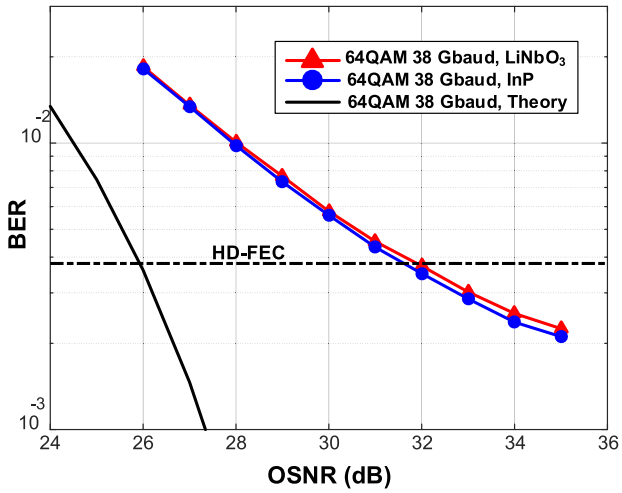

Fig. 5. 38 Gbaud, 64 QAM, BER versus OSNR system performance as a function of modulator platform.

V. Conclusion

We demonstrated 400G transmission using an InP-based DP-IQM on a single carrier including the required overhead at different modulation formats and symbol rates, namely 16-QAM at 56 Gbaud and 64-QAM at both 38 and 43 Gbaud. Transmission of the 56 Gbaud 16-QAM signal needs lower OSNR and can propagate over longer distances (more than 500 km) compared to 64-QAM signals at lower symbol rates. These results show the viability of using InP-based DP-IQM to meet 400G transmission system requirements.

References

[1] J. Zhang, J. Yu, Z. Jia, and H.-C. Chien, "400 G transmission of super-Nyquist-filtered signal based on single-carrier 110-GBaud PDM QPSK with 100-GHz grid," *J. Lightw. Technol.*, vol. 32, no. 19, pp. 3239–3246, Oct. 1, 2014.

[2] J. H. Ke, Y. Gao, and J. C. Cartledge, "400 Gbit/s single-carrier and 1 Tbit/s three-carrier superchannel signals using dual polarization 16-QAM with look-up table correction and optical pulse shaping," *Opt. Exp.*, vol. 22, no. 1, pp. 71–84, 2014.

[3] R. Rios-Müller *et al.*, "Spectrally-efficient 400-Gb/s single carrier transport over 7 200 km," *J. Lightw. Technol.*, vol. 33, no. 7, pp. 1402–1407, Apr. 1, 2015.

[4] F. Buchali, A. Klekamp, L. Schmalen, and T. Drenski, "Implementation of 64QAM at 42.66 GBaud using 1.5 samples per symbol DAC and demonstration of up to 300 km fiber transmission," presented at the OFC, San Francisco, CA, USA, 2014.

[5] T. J. Xia *et al.*, "Transmission of 400G PM-16QAM channels over long-haul distance with commercial all-distributed Raman amplification system and aged standard SMF in field," presented at the OFC, San Francisco, CA, USA, 2014.

[6] G. Raybon *et al.*, "Single-carrier 400G interface and 10-channel WDM transmission over 4,800 km using all-ETDM 107-Gbaud PDM-QPSK," presented at the OFC, Anaheim, CA, USA, 2013.

[7] S. Chandrasekhar, X. Liu, P. J. Winzer, J. E. Simsarian, and R. A. Griffin, "Compact all-InP laser-vector-modulator for generation and transmission of 100-Gb/s PDM-QPSK and 200-Gb/s PDM-16-QAM," *J. Lightw. Technol.*, vol. 32, no. 4, pp. 736–742, Feb. 15, 2014.

[8] G. Letal *et al.*, "Low loss InP C-band IQ modulator with 40 GHz bandwidth and 1.5 V $V\pi$" presented at the OFC, Los Angeles, CA, USA, 2015.

[9] T. Tatsumi *et al.*, "A compact low-power 224-Gb/s DP-16QAM modulator module with InP-based modulator and linear driver ICs," presented at the OFC, San Francisco, CA, USA, 2014.

[10] M. Smit *et al.*, "An introduction to InP-based generic integration technology," *Semicond. Sci. Technol.*, vol. 29, no. 8, pp. 1–41, 2014.

[11] N. Kikuchi, R. Hirai, and Y. Wakayama, "High-speed optical 64QAM signal generation using InP-based semiconductor IQ modulator," presented at the OFC, San Francisco, CA, USA, 2014.

[12] S. J. Savory, "Digital coherent optical receivers: Algorithms and subsystems," *IEEE J. Sel. Topics Quantum Electron.*, vol. 16, no. 5, pp. 1164–1179, Sep./Oct. 2010.

[13] S. J. Savory, "Digital filters for coherent optical receivers," *Opt. Exp.*, vol. 16, no. 2, pp. 804–817, 2008.

[14] P. Ciblat and M. Ghogho, "Blind NLLS carrier frequency-offset estimation for QAM, PSK, and PAM modulations: Performance at low SNR," *IEEE Trans. Commun.*, vol. 54, no. 10, pp. 1725–1730, Oct. 2006.

[15] Y. Wang, E. Serpedin, and P. Ciblat, "An alternative blind feedforward symbol timing estimator using two samples per symbol," *IEEE Trans. Commun.*, vol. 51, no. 9, pp. 1451–1455, Sep. 2003.

[16] Y. Han and G. Li, "Coherent optical communication using polarization multiple-input-multiple-output," *Opt. Exp.*, vol. 13, no. 19, pp. 7527–7534, 2005.

[17] I. Fatadin, D. Ives, and S. J. Savory, "Compensation of frequency offset for differentially encoded 16- and 64-QAM in the presence of laser phase noise," *IEEE Photon. Technol. Lett.*, vol. 22, no. 3, pp. 176–178, Feb. 1, 2010.

[18] P. J. Winzer and R. Essiambre, "Advanced optical modulation formats," in *Optical Fiber Telecommunications volumes V & B*, I. P. Kaminow, T. Li, and A. E. Willner, Eds. New York, NY, USA: Elsevier, 2008.

[19] H. Yamazaki, T. Goh, T. Hashimoto, A. Sano, and Y. Miyamoto, "Generation of 448-Gbps OTDM-PDM-16QAM signal with an integrated modulator using orthogonal CSRZ pulses," presented at OFC, Los Angeles, CA, USA, 2015.

[20] J. K. Fischer *et al.*, "8 × 448-Gb/s WDM transmission of 56-GBd PDM 16-QAM OTDM signals over 250-km ultralarge effective area fiber," *IEEE Photon. Technol. Lett.*, vol. 23, no. 4, pp. 239–241, Feb. 15, 2011.

[21] D. Rafique, A. Napoli, S. Calabro, and B. Spinnler, "Digital preemphasis in optical communication systems: On the DAC requirements for terabit transmission applications," *J. Lightw. Technol.*, vol. 32, no. 19, pp. 3247–3256, Oct. 1, 2014.